

# Supramolecular Routes to Hierarchical Structures: Comb-Coil Diblock Copolymers Organized with Two Length Scales

J. Ruokolainen,<sup>†</sup> M. Saariaho, and O. Ikkala\*

Department of Engineering Physics and Mathematics, Helsinki University of Technology,  
P.O. Box 2200, FIN-02015 HUT, Espoo, Finland

G. ten Brinke\*,<sup>‡</sup>

Department of Polymer Science, Materials Science Center, University of Groningen, Nijenborgh 4,  
9747 AG Groningen, The Netherlands

E. L. Thomas

Department of Materials Science and Engineering, Massachusetts Institute of Technology,  
Cambridge, Massachusetts 02139

M. Torkkeli and R. Serimaa

Department of Physics, University of Helsinki, P.O. Box 9, FIN-00014 Helsinki, Finland

Received February 9, 1998

**ABSTRACT:** We show that polymeric materials characterized by two length scales are obtained if diblock copolymers are mixed with amphiphilic selective solvents, leading to self-organization which combines the "block copolymer length scale" with a much shorter "nanoscale". In this work, the amphiphilic compound is 3-*n*-pentadecylphenol (PDP) which is hydrogen-bonded to the pyridine group of polystyrene-*block*-poly(4-vinylpyridine), i.e., PS-*b*-P4VP. The molecular architecture resembles comb-coil diblock copolymers A-*block*-(B-*graft*-C) but is obtained using the supramolecular assembly route. The structures were determined with a combination of transmission electron microscopy and small-angle X-ray scattering. On the block copolymer scale (300 Å range), the PS blocks are microphase-separated from the P4VP-(PDP)<sub>x</sub> blocks, where *x* denotes the ratio between the number of phenol and pyridine groups. For PS-*b*-P4VP block copolymers having a spherical morphology and P4VP as the minority component, the structure of PS-*b*-P4VP(PDP)<sub>x</sub> changes from spherical to hexagonal and further to lamellar as a function of the amount of PDP added. For all comb-coil diblock copolymer morphologies, the P4VP(PDP)<sub>x</sub> domains are further "nanophase-separated" into lamellar structures due to microphase separation of the comb copolymer-like complex between P4VP and PDP. The morphology diagram is presented for stoichiometric conditions (*x* = 1), using a range of different PS-*b*-P4VP block copolymers.

## 1. Introduction

It is expected that polymeric materials with order at several length scales offer possibilities for new technologies and applications.<sup>1</sup> The domains can be selectively equipped with electrical, optical, or other functionalities, and using the self-organizing aspects of structure formation, the functionalities may be switched on and off by order–disorder or order–order transitions.<sup>2</sup> Therefore, it becomes relevant to develop sufficiently simple and systematic concepts for hierarchical phases and to tailor transition temperatures to useful temperatures which allow switching.

A variety of ordered structures can be constructed using block copolymers, depending on the number of blocks, their volume fraction, chain flexibility, architecture, and the extent of repulsion between the chemically connected blocks.<sup>3,4</sup> The simplest example is provided by AB, ABA, and (AB)<sub>n</sub> block copolymers consisting of two different flexible (coil-like) polymer blocks with the classical body-centered cubic (bcc), hexagonal cylinder, and lamellar phases.<sup>4</sup> These block copolymer morphologies are characterized by a basic periodicity, which

is usually in the 100–1000 Å range. Recently a number of different, more complex structures have been found as well: the gyroid structure,<sup>5–7</sup> the hexagonally modulated lamellae, and the hexagonally perforated layers.<sup>8,9</sup> Because of the polymeric nature of the blocks, the material under normal conditions is in the microphase-separated state and considerable ingenuity is required to reduce the order–disorder temperatures to fall inside the range of 20–150 °C. Furthermore, three different flexible polymer blocks can be combined to form ABC triblock copolymers where more complicated structures can be obtained.<sup>10–14</sup> Various micellar and core–shell morphologies, as well as morphologies for which the domain boundaries of lamellar or cylindrical morphologies have been decorated with a third phase, have been reported so far.

A different variant to obtain self-organized structures consists of block copolymers with conformational asymmetry between the blocks, for example, when one of the blocks is liquid crystalline (LC).<sup>15,16</sup> In this case, liquid crystallinity and block copolymer microphase separation both contribute to the structure formation and complicated self-organization has been reported.<sup>17–19</sup> Adams and Gonski<sup>20</sup> introduced diblock copolymers in which one block contains mesogenic side groups chemically attached to the backbone, whereas the other block

<sup>†</sup> Also Institute of Biotechnology, Electron Microscopy, University of Helsinki, P.O. Box 56, FIN-00014 Helsinki, Finland.

<sup>‡</sup> Also Helsinki University of Technology.

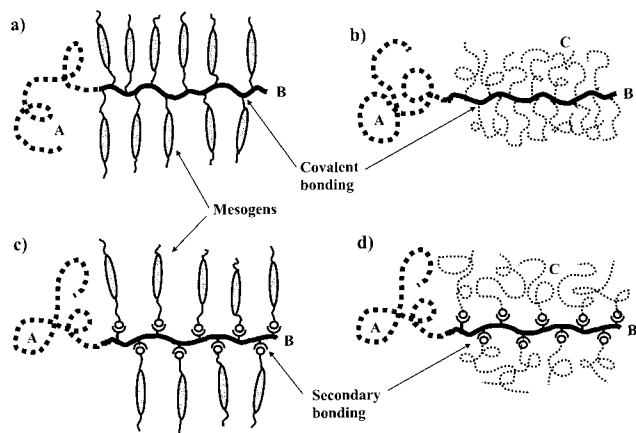


**Figure 1.** Schematic presentation of polymer architectures: (a) LC-coil diblock copolymer; (b) Comb-coil diblock copolymer A-block-(B-graft-C); (c) LC-coil diblock copolymer with the mesogens bonded by secondary interactions; (d) Comb-coil diblock copolymer with the side chains bonded by secondary interactions, thus resembling A-block-(B-graft-C).

is coil-like. The structure formation and synthesis of "LC-coil block copolymers" or "rod-coil polymers" have recently been subject to intense research.<sup>21–28</sup> Simultaneous microphase separated lamellar, cylindrical, and spherical structures at the 100–1000 Å length scale and smectic ordering at a shorter length scale have been reported.<sup>28,29</sup>

In this paper, we introduce a novel and particularly simple way to construct polymeric structures with two length scales. Two observations guided our work:

(1) In the previous studies on LC coils, conformational asymmetry has been achieved based on, for example, the smectic order caused by the covalently bonded mesogenic side groups (see Figure 1a). A different mechanism to achieve mesomorphic structure within one domain will benefit from *another level* of block copolymeric microphase separation (see Figure 1b). It is, however, a further example of a complicated A-block-(B-graft-C) architecture of three chemically connected flexible units and does not offer any simpler synthesis as compared with the LC-coil diblock copolymers.

(2) Instead of covalent bonds, it suffices to bond the side groups by tailored secondary interactions. Different routes to mesomorphic polymer complexes have been reported by bonding suitable side groups to polymers by ionic interaction, hydrogen bonding, molecular recognition, or coordination bonding.<sup>30–35</sup> For example, Figure 1c shows the scheme when a mesogenic side group is complexed to a polymer chain. Likewise, flexible side groups can be complexed with homopolymers using ionic interactions<sup>36–40</sup> and hydrogen bonding<sup>41–46</sup> to yield mesomorphic structures.

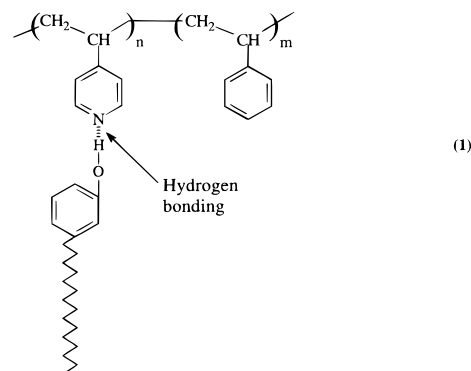
Poly(4-vinyl pyridine) (P4VP) hydrogen-bonded to PDP is a model system which behaves like a comb copolymer B-graft-C, exhibiting a mesomorphic state at low temperatures followed by an order–disorder transition at ca. 60 °C, as manifested by small-angle X-ray scattering (SAXS) and rheology.<sup>41,43</sup> These nanoscale structures have recently been imaged directly using a longer phenol, i.e., nonadecylphenol.<sup>42</sup> The order–disorder transition temperature can be tailored systematically by varying the alkyl chain length and composition.<sup>44</sup> Through manipulation of the strength of the hydrogen bond and the magnitude of the repulsion, order–disorder transition temperatures can be obtained in the range of 50–200 °C. At the same time, the long

**Table 1.** Characteristics of the PS-*b*-P4VP(PDP)<sub>1.0</sub> Systems Used

composition	PS (g/mol)	P4VP (g/mol)	$M_w/M_n$	P4VP(PDP) <sub>1.0</sub> weight fraction
S-(4VP-PDP)-0.15	41 400	1 900	1.07	0.152
S-(4VP-PDP)-0.25	34 000	2 900	1.07	0.250
S-(4VP-PDP)-0.29	35 500	3 680	1.06	0.288
S-(4VP-PDP)-0.35	40 000	5 600	1.09	0.353
S-(4VP-PDP)-0.45	238 100	49 500	1.23	0.448
S-(4VP-PDP)-0.49	32 900	8 080	1.06	0.489
S-(4VP-PDP)-0.62	31 900	13 200	1.08	0.617
S-(4VP-PDP)-0.79	21 400	20 700	1.13	0.790
S-(4VP-PDP)-0.92	18 600	55 800	1.26	0.921

period of the structure can be varied between 20 and 60 Å, which is an order of magnitude smaller than the long period of conventional block copolymers. Next, such a comb-shaped polymer–amphiphile complex can be selected to form one block of a diblock copolymer (see Figure 1d).

The combination of these two different ways of obtaining ordered structures makes it possible to create structures-within-structures in a straightforward way. This will be illustrated on the basis of simple model systems consisting of a mixture of a diblock copolymer of polystyrene (PS) and P4VP with PDP, see eq 1.



The hierarchical structures will be investigated using SAXS in combination with transmission electron microscopy (TEM). We will also investigate the phase transitions and discuss the order–disorder transition of the polymer–amphiphile complex.

## 2. Experimental Section

**Materials.** Nine different diblock copolymers of polystyrene and poly(4-vinyl pyridine) (PS-*b*-P4VP) were used (Polymer Source, Inc.); see Table 1 for the block lengths and polydispersities. Also pure polystyrene ( $M_n = 47\,500$ ;  $M_w/M_n = 1.03$ ) was acquired from Polymer Source, Inc. The polymers were used without further purification. PDP was purchased from Pfaltz & Bauer (purity 97%). The main remaining impurity was due to alkyl phenols of different alkyl chain lengths.

**Sample Preparation.** First, PS-*b*-P4VP samples were dried in a vacuum at 60 °C and PDP at 40 °C for at least 24 h. PS-*b*-P4VP(PDP)<sub>x</sub> were prepared by dissolving PS-*b*-P4VP and PDP in analysis-grade chloroform. The concentration of polymer in the solvent was kept low (less than 1 wt %) to ensure homogeneous complex formation. Subsequently, the solvent was evaporated very slowly at ca. 40 °C. The final drying took place in a vacuum at 60 °C for at least 2 days. Then, the samples were annealed for one week at 120 °C under nitrogen. PS-*b*-P4VP(PDP)<sub>1.0</sub>/PS blends were similarly prepared from a chloroform solution.

**Small-Angle X-ray Scattering.** A sealed fine focus Cu X-ray tube was used in point-focusing mode. The Cu K $\alpha$  ( $\lambda = 1.542$  Å) radiation is monochromatized with Ni filter and a totally reflecting glass block (Huber small-angle chamber 701).

The scattered radiation is detected in the horizontal (beam width) direction by a linear one-dimensional proportional counter (MBraun OED-50M). Two separate temperature scans were made to cover both length scales. For the 10–100 Å range, the sample to detector distance was 165 mm, and the instrumental function had full width at half-maximum =  $0.037 \text{ Å}^{-1}$  in the vertical direction and  $0.0072 \text{ Å}^{-1}$  in the horizontal direction. For the larger range of 100–1000 Å, the sample-to-detector distance was 1170 mm, and the instrumental function was set to  $0.019 \text{ Å}^{-1}$  in the vertical direction and  $0.0026 \text{ Å}^{-1}$  in the horizontal direction. Thus, the scattering curves appear practically unsmearred in the first case, but in the latter case, a slight smearing and shifting of the peaks has to be taken into account.

**Infrared Spectroscopy.** Infrared spectra were obtained using a Nicolet 730 FTIR spectrometer. Samples were prepared by solvent casting from chloroform onto potassium bromide crystals. To prevent evaporation of pentadecylphenol during temperature sweeps to elevated temperatures, an additional KBr layer was deposited on top of the sample to achieve a sealed sample.

**Electron Microscopy.** Bulk samples of PS-*b*-P4VP(PDP)<sub>*x*</sub> for TEM characterization were embedded in epoxy and cured at 60 °C overnight. Ultrathin sections were cut from the embedded specimen using a Reichert Ultracut E ultramicrotome and a diamond knife at room temperature. Sections were picked up on 600 mesh copper grids, and to enhance contrast, the microtomed sections were stained in the vapor of I<sub>2</sub> crystals. Bright field TEM was performed on either a JEOL-1200EX or a JEOL-2000FX transmission electron microscope with a tungsten filament and a LaB<sub>6</sub> source, respectively. Microscopes were operated at an accelerating voltage of 60 and 100kV.

### 3. Results and Discussion

We start our discussion about the development of supramolecular polymeric materials which order at two different length scales by considering the system PS-*b*-P4VP(PDP)<sub>1.0</sub> [sample S-(4VP-PDP)-0.35 in Table 1], obtained by combining the diblock copolymer PS-*b*-P4VP with a stoichiometric amount of PDP (i.e., an equal number of pyridine and phenol groups:  $x = 1.0$ ). The amount of P4VP(PDP)<sub>1.0</sub> material for this particular system is approximately 35 wt %, which suggests that at the block copolymer level the system will microphase-separate into a lamellar structure of alternating PS and P4VP(PDP)<sub>1.0</sub> layers.

**3.1. Lamellar-within-Lamellar Structure. Small-Angle X-ray Scattering and TEM.** From our previous work on pure P4VP(PDP)<sub>*x*</sub> systems,<sup>41–43</sup> we know that in these homopolymer–amphiphile systems an ordered lamellar structure occurs below approximately 60 °C, this being the order–disorder transition temperature (ODT) for  $x = 1.0$ . The structure consists of alternating layers of nonpolar alkyl chains and polar P4VP–phenol material.<sup>47</sup> The volume fraction of both layers is approximately the same, and in the corresponding SAXS data, the second-order peak is therefore systematically absent. The second-order peak becomes visible below ca. 25 °C because of the crystallization of the outer parts of the alkyl “side chains”,<sup>41,48</sup> which alters the symmetry.

Figure 2 shows the corresponding temperature-dependent SAXS data for the PS-*b*-P4VP(PDP)<sub>1.0</sub> comb-coil diblock copolymer system (sample S-(4VP-PDP)-0.35 in Table 1). The peak at  $k \approx 0.18 \text{ Å}^{-1}$  corresponds to the small length scale lamellar structure. As for the homopolymer complex, the second-order peak is not observable near 40 °C. When heated, the SAXS data show a strong reduction in height of this peak at

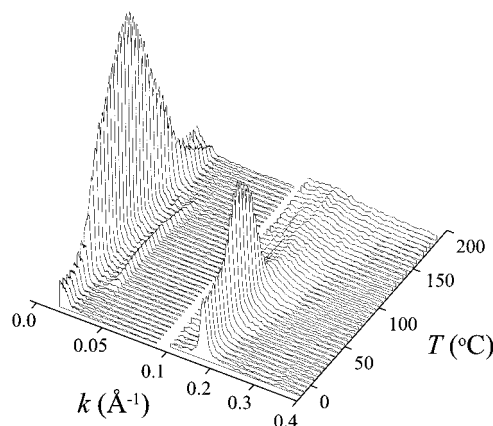


**Figure 2.** Temperature-dependent SAXS data for PS-*b*-P4VP-(PDP)<sub>1.0</sub> [sample S-(4VP-PDP)-0.35] during heating at 2 °C/min. Block copolymer scale: The peak at  $k = 0.0195 \text{ Å}^{-1}$  (and a second-order peak at twice this value) is due to PS and P4VP-(PDP)<sub>1.0</sub> lamellae. Nanoscale: The peak at  $k = 0.18 \text{ Å}^{-1}$  is due to the lamellar order of nonpolar pentadecyl tails, and polar groups is due to the internal structure within the P4VP(PDP)<sub>1.0</sub> lamellae.  $T_{\text{ODT}} \approx 60 \text{ °C}$ .

around 60 °C, because of the ODT. Only a shallow correlation hole peak remains above this temperature.<sup>49</sup> Below ca. 25 °C, the peak intensity drops because of the crystallization of the alkyl side chains. All of these observations pertaining to the P4VP-containing domains are analogous to the homopolymer P4VP(PDP)<sub>1.0</sub> system. A slight difference is the absence of a small second-order peak for the crystallized sample (i.e., for  $T < 25 \text{ °C}$ ). It seems to be related to the fact that the P4VP-(PDP)<sub>1.0</sub> layers are confined between *glassy* PS layers because in separate SAXS measurements on a corresponding rubbery polybutadiene (PB) containing comb-coil diblock copolymer system, i.e., PB-*b*-P4VP(PDP)<sub>1.0</sub>, the second-order peak appeared on crystallization.

That we are really dealing with a lamellar-within-lamellar structure is confirmed by the occurrence of a SAXS peak at  $k \approx 0.0195 \text{ Å}^{-1}$  together with the second-order peak, indicating lamellar order at a long period of ca. 320 Å. The SAXS data presented in Figure 2 have been recorded during a slow heating at 2 °C/min but similar results are observed during cooling, apart from a minor hysteresis. Therefore the SAXS data indicates reversibility. At elevated temperatures, the second-order peak vanishes, and the intensity of the block copolymer main peak is strongly reduced. Although this is not the main topic of the present paper, it is of interest because it is related directly to the thermoreversibility of the hydrogen bonding.

However, before discussing this point, we will first consider the results based on TEM. From the previous studies, we know that pure P4VP, as well as slightly cross-linked P4VP, forms a lamellar structure when complexed with PDP.<sup>41,43,50</sup> This structure has been imaged by TEM for the first time using the somewhat longer alkylphenol, i.e., nonadecylphenol (NDP), leading to the complex P4VP(NDP)<sub>1.0</sub>.<sup>42</sup> In this work, P4VP-(PDP)<sub>1.0</sub> forms the comb block of the comb-coil diblock copolymer, and its lamellar organization with a long period of 36 Å is located inside the P4VP(PDP)<sub>1.0</sub> layers. This structure-within-structure morphology has also been imaged by TEM using NDP.<sup>2</sup> In Figure 3, we present the first TEM picture of a lamellar-within-lamellar structure using the shorter alkylphenol, i.e., for PS-*b*-P4VP(PDP)<sub>1.0</sub>. The figure demonstrates



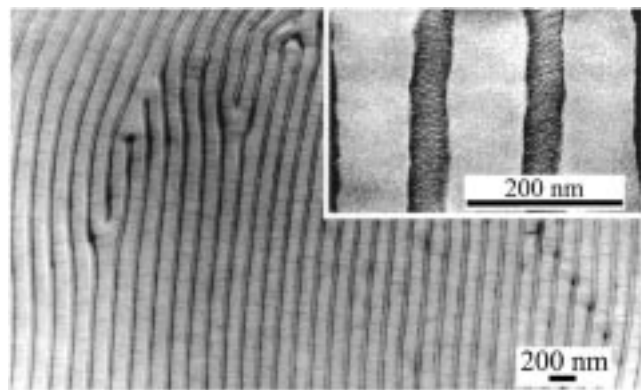


**Figure 3.** TEM of PS-*b*-P4VP(PDP)<sub>1.0</sub> [sample S-(4VP-PDP)-0.45] showing the lamellar-inside-lamellar structure with the mutually approximately perpendicular orientations.

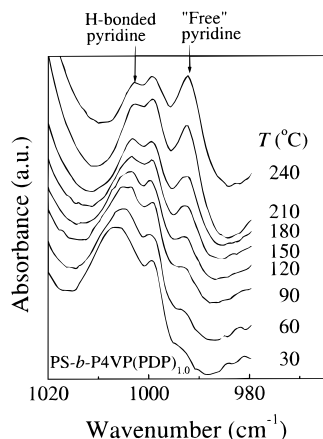


**Figure 4.** Temperature-dependent FTIR of PS-*b*-P4VP-(PDP)<sub>1.0</sub> [sample S-(4VP-PDP)-0.35]. Free pyridine, 993 cm<sup>-1</sup>; hydrogen bonded pyridine, 1008 cm<sup>-1</sup>; 3-phenol, 999 cm<sup>-1</sup>.

that, as in the case of NDP, both lamellar structures are oriented approximately perpendicular to each other.

The reduced strength of the hydrogen bonding at elevated temperatures can be studied using FTIR. In the case of PS-*b*-P4VP(PDP)<sub>1.0</sub>, characteristic absorption bands are shown in Figure 4 for the free and hydrogen-bonded pyridine groups, i.e., 993 and 1005–1010 cm<sup>-1</sup>, respectively. Note that an overlapping peak due to PDP at 999 cm<sup>-1</sup> complicates a quantitative analysis. At low temperatures, most of the pyridine groups are hydrogen-bonded. By contrast, considerable decoupling is observed at high temperatures, such as above 150 °C. It was separately observed that homopolymer PS becomes soluble in PDP for  $T > \text{ca. } 130\text{ }^{\circ}\text{C}$ . As demonstrated, at these high temperatures, a significant proportion of the hydrogen bonds between PDP and P4VP are broken. In PS-*b*-P4VP(PDP)<sub>1.0</sub> samples, the weight fraction of PDP is generally rather large, i.e., 26 wt % in this particular case. Hence, a substantial amount of PDP will start to migrate into the PS layer, as PDP becomes a relatively *nonselective* solvent for PS-*b*-P4VP. If PDP were evenly distributed, the weight fraction of the P4VP-containing phase would be about 12 wt % (reduced from 35 wt %). Therefore one possible explanation of the SAXS data is that PS-*b*-P4VP forms a spherical phase with a relatively poor order in the PDP solvent background. The other option, that the high-temperature peak is due to the correlation hole effect of the *homogeneous* state of PS-*b*-P4VP(PDP)<sub>1.0</sub> can easily be dismissed. Dilution by nonselective solvents has recently been discussed both theoretically<sup>51–53</sup> and experimentally.<sup>54,55</sup> In the sim-

plest approximation, a reduction of the total polymer volume fraction to  $\varphi < 1$  modifies the Leibler criterion<sup>3,54</sup> for the ODT to

$$(\chi N)_{\text{ODT}} = \frac{F(f)}{2} \xrightarrow{\varphi} (\varphi^{1.60} \chi N)_{\text{ODT}} = \frac{F(f)}{2} \quad (2)$$

where  $f$  is the composition of the block copolymer. For the present PS-*b*-P4VP,  $f$  is selected as the volume fraction of the P4VP-containing block which leads to  $f \approx 0.12$ , and  $F(f)$  is a constant depending on  $f$ , approximately 80 in our case. Taking  $N = 430$  and  $\varphi \approx 0.74$ , this would require  $\chi \approx 0.15$  near an ODT. The measured value has been found to be even larger than 1.0,<sup>56</sup> making PS-*b*-P4VP a candidate for the super-strong segregation regime.<sup>56,57</sup> The above reasoning does not easily suggest the identification of the high-temperature phase as a homogeneous phase.

Efforts to image the high-temperature structure by TEM have been undertaken, and samples quenched from +200 to -150 °C using liquid propane indeed showed a morphology consisting of poorly ordered short cylinders, which readily transformed back into lamellar morphology upon annealing at 120 °C. However, it is not clear whether even the present quenching was sufficiently fast to arrest the actual high-temperature structure. The presence of a large amount of evenly distributed PDP makes it a low  $T_g$  material. In a related study involving the more complicated charged PS-*b*-P4VP(MSA)<sub>1.0</sub>(PDP)<sub>1.0</sub> system [here methane sulfonic acid (MSA) protonates the pyridine rings, and the PDP molecules hydrogen bond to the sulfonates of MSA], the transition from a lamellar to cylindrical structure due to the diffusion of PDP into the PS domains was readily observable upon heating in the SAXS measurements.<sup>2</sup> In this case, PDP becomes even a selective solvent for PS at high temperatures, being expelled almost completely from the P4VP(MSA)<sub>1.0</sub> phase because of macrophase separation. Hence, thermoreversibility of the hydrogen bonding in combination with the high-temperature miscibility of PS and PDP has a pronounced influence on the high-temperature morphology. However, as far as the precise sequence of structural transitions is concerned for the present system, the SAXS and TEM data are still inconclusive.

**3.2. Structure-within-Structures.** In the previous section, we discussed one particular system with a self-organized lamellar-within-lamellar structure. But it is obvious that a variety of different hierarchical structures may be obtained along the same lines. Here we will limit ourselves to P4VP(PDP) <sub>$x$</sub>  being the supramolecular block of a diblock copolymer with PS. Within this class of systems, there are two different ways to manipulate the self-organization. We can either change the composition of the PS-*b*-P4VP diblock copolymer and keep fixed  $x$  or, alternatively, vary the amount of PDP added (i.e., vary  $x$ ) for a fixed diblock copolymer. Both possibilities offer a means to systematically change the amount of P4VP(PDP) (or PS) present in the system. Homopolymer complexes P4VP(PDP) <sub>$x$</sub>  form low-temperature lamellar structures for  $0.5 \leq x \leq 1.5$ . For smaller values of  $x$ , the system vitrifies before an order-disorder transition occurs, whereas for larger values of  $x$ , crystallization of the alkyl material intervenes.<sup>41,43,48</sup> Hence, both ways allow tailoring of the large length scale structure, whereas the internal structure of the P4VP-(PDP) domains will be lamellar.

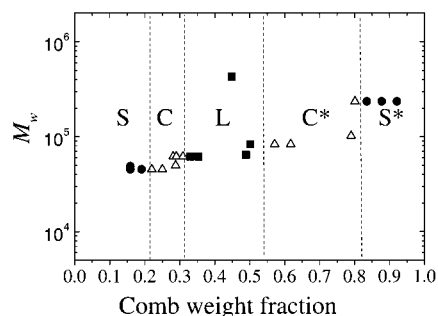


**Figure 5.** Morphology diagram of PS-*b*-P4VP(PDP)<sub>1.0</sub> illustrating the block copolymer level structures. L = Lamellar; C, C\* = cylindrical; and S, S\* = spherical morphology.

**Influence of PS-*block*-P4VP Composition.** In this section, we will concentrate on stoichiometric conditions, i.e., PS-*b*-P4VP(PDP)<sub>1.0</sub> and discuss phase behavior using the set of block copolymers collected in Table 1. Figure 5 presents the block copolymer morphology diagram, as determined by TEM, of the comb-coil diblock copolymers as a function of the comb [i.e., P4VP-(PDP)<sub>1.0</sub>] weight fraction. Besides the nine different block copolymer systems, the diagram also contains points obtained by adding monodisperse polystyrene of molar mass 47.500 g/mol to PS-*b*-P4VP(PDP)<sub>1.0</sub>. The morphology diagram represents the structures as a function of weight fraction rather than volume fraction of P4VP(PDP)<sub>1.0</sub>. However, the densities of the two phases are only slightly different (literature value for PS, 1.047 g/cm<sup>3</sup>; measured value for P4VP(PDP)<sub>1.0</sub>, 0.98 g/cm<sup>3</sup>), and the use of volume fractions will not substantially change the appearance of the diagram. Compared to the morphology diagram of simple diblock copolymers in the strong segregation regime, this diagram shows a strong asymmetry characterized by a strongly enhanced stability of the cylindrical morphology at the high P4VP(PDP)<sub>1.0</sub> end, i.e., cylinders of PS (denoted as C\* in Figure 5). Of course, some kind of asymmetry has to be expected given the asymmetric nature of the comb-coil diblock copolymer. Similarly, Fischer and Poser<sup>16</sup> describe a strongly enhanced stability of the spherical morphology at both ends of the composition axis for LC-coil diblock copolymers consisting of the side chain liquid crystalline poly(2-(3-cholesteryl-oxycarbonyloxy)ethyl methacrylate) and polystyrene.

**Influence of  $x$  on Morphology of PS-*block*-P4VP-(PDP) <sub>$x$</sub> .** For flexible diblock copolymers in the strong segregation regime, the transition from spherical to cylindrical and further to lamellar structure occurs for values of the block copolymer composition  $f$  approximately given by 0.16 and 0.32, respectively. These numbers follow from what is essentially a volume-interface argument in which the overall stretching of the chains is assumed to remain approximately the same during structural transformation.<sup>58</sup> This concept equally applies to diblock copolymers swollen by selective solvents. At low temperatures, PDP forms a strong hydrogen bond with P4VP and as such acts as a selective amphiphilic solvent for PS-*b*-P4VP. For a PS-*b*-P4VP copolymer, which is originally in the spherical phase such as sample S-(4VP-PDP)-0.35 (Table 1), the addition of PDP is thus expected to induce structural transformations, in analogy with block copolymer-selective solvent systems.<sup>59,60</sup> That this is really the case is demonstrated by TEM micrographs of PS-*b*-P4VP-(PDP) <sub>$x$</sub>  for  $x = 0, 0.5$ , and  $1.0$ , presented in Figure 6.

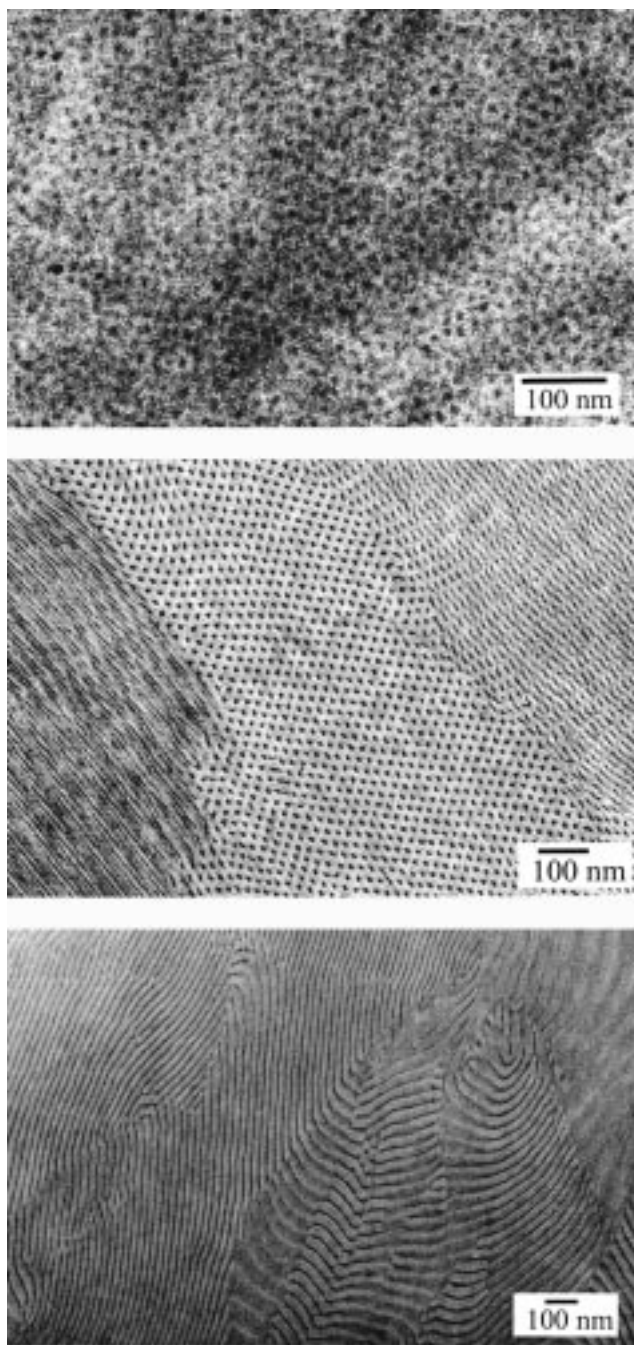


**Figure 6.** TEM micrographs showing the block copolymer scale structures of PS-*b*-P4VP(PDP) <sub>$x$</sub>  for sample S-(4VP-PDP)-0.35: (a) spherical bcc morphology for  $x = 0.0$ , (b) cylindrically hexagonal morphology for  $x = 0.5$ , and (c) lamellar morphology for  $x = 1.0$ .

They correspond to P4VP(PDP) <sub>$x$</sub>  weight fractions of 0.12, 0.26, and 0.35 and exhibit the expected spherical, cylindrical, and lamellar morphologies, respectively. No signs of more complicated structures, such as the gyroid structure, have been found. This does not come as a real surprise because it is commonly believed that in the strong segregation regime the phase diagram retains only the classical phases,<sup>61</sup> although Antonietti and co-workers<sup>62</sup> recently observed that block copolymers with very incompatible blocks exhibit new mesophases. At room temperature, our systems are most probably also in the strong segregation regime; one of the three Flory-Huggins interaction parameters involved, i.e., between PS and P4VP, even exceeds 1.0.<sup>56</sup>



#### 4. Concluding Remarks

In this work, we demonstrated a simple supramolecular way of constructing self-organizing comb-coil diblock copolymers with two length scales by combining diblock copolymers with hydrogen-bonding amphiphiles. The concept allows a rich variety of morphologies and phase transitions by modifying the block lengths, the amount of the amphiphiles, their alkyl chain lengths, and the strength of the hydrogen bonding. In this work, we determine the morphologies of PS-*b*-P4VP(PDP)<sub>1.0</sub>. We know from separate TEM studies on mixtures of homopolymer P4VP and PDP that these comb copolymerlike molecules form nanoscale lamellar structures with a long period of ca. 40 Å. SAXS and TEM demonstrate that these nanoscale structures also are formed within the block copolymer scale structures, i.e., in the confined geometry. From the TEM results presented here and from a TEM study on PS-*b*-P4VP-(NDP)<sub>1.0</sub> systems,<sup>63</sup> we found that the lamellar-within-lamellar morphology is characterized by a mutually approximately perpendicular orientation. This result is also confirmed by preliminary SAXS data on shear-oriented samples.<sup>64</sup>

The richness of the phase behavior can be appreciated by summarizing the sequence of transitions in the case of PS-*b*-P4VP(PDP)<sub>1.0</sub> [sample S-(4VP-NDP)-0.35] upon heating:

-At  $T < \text{ca. } 25^\circ\text{C}$ , the coil-like PS and the comb-like P4VP(PDP)<sub>1.0</sub> form alternating layers with a long period of 320 Å. The latter layers have another nanoscale lamellar structure consisting of alternating polar moieties (containing the P4VP chains and the phenolic rings) and nonpolar *crystallized* pentadecyl tails with a long period of 36 Å. The two lamellar structures are perpendicular to each other.

-At  $25^\circ\text{C}$ , the side chain crystalline structures melt.

-At  $T_{\text{ODT}} \approx 60^\circ\text{C}$ , the P4VP(PDP)<sub>1.0</sub> block undergoes an ODT.

-At  $\text{ca. } 60^\circ\text{C} < T < 85^\circ\text{C}$ , the P4VP(PDP)<sub>1.0</sub> lamellae have a disordered internal structure and are confined by the glassy PS lamellae. Hydrogen bonding still suffices to keep P4VP(PDP)<sub>1.0</sub> essentially as comb copolymer-like molecules.

-At  $85^\circ\text{C}$ , the PS lamellae become rubbery because of the glass transition.

-Around  $130\text{--}150^\circ\text{C}$ , the hydrogen bonding between PDP and P4VP is strongly reduced, and in addition, PDP becomes soluble in PS. These two factors show that PDP gradually becomes a nonselective solvent for PS-*b*-P4VP inducing morphological transitions that are not fully clarified yet.

**Acknowledgment.** This work has been supported by the Finnish Academy, the Technology Development Centre (Finland) and Neste Foundation. This work was supported in part by the MRSEC Program of the National Science Foundation under Award Number DMR 94-0334. We thank the Center for Materials Science and Engineering electron microscopy facility at the Massachusetts Institute of Technology.

#### References and Notes

- Muthukumar, M.; Ober, C. K.; Thomas, E. L. *Science* **1997**, *277*, 1225.
- Ruokolainen, J.; Mäkinen, R.; Torkkeli, M.; Mäkelä, T.; Serimaa, R.; ten Brinke, G.; Ikkala, O. *Science* **1998**, *280*, 557.
- Leibler, L. *Macromolecules* **1980**, *13*, 1602.
- Bates, F. S.; Fredrickson, G. H. *Annu. Rev. Phys. Chem.* **1990**, *41*, 525.
- Hajduk, D. A.; Harper, P. E.; Gruner, S. M.; Honeker, C. C.; Kim, G.; Thomas, E. L.; Fetters, L. J. *Macromolecules* **1994**, *27*, 4063.
- Schulz, M. F.; Bates, F. S.; Almdal, K.; Mortensen, K. *Phys. Rev. Lett.* **1994**, *73*, 86.
- Hajduk, D. A.; Harper, P. E.; Gruner, S. M.; Honeker, C. C.; Thomas, E. L.; Fetters, L. J. *Macromolecules* **1995**, *28*, 2570.
- Hamley, I. W.; Koppi, K. A.; Rosedale, J. H.; Bates, F. S.; Almdal, K.; Mortensen, K. *Macromolecules* **1993**, *26*, 5959.
- Hajduk, D. A.; Takenouchi, H.; Hillmyer, M. A.; Bates, F. S.; Vigild, M. E.; Almdal, K. *Macromolecules* **1997**, *30*, 3788.
- Gido, S. P.; Schwark, D. W.; Thomas, E. L.; do Carmo Concalves, M. *Macromolecules* **1993**, *26*, 2636.
- Auschra, C.; Stadler, R. *Macromolecules* **1993**, *26*, 2171.
- Stadler, R.; Auschra, C.; Beckmann, J.; Krappe, U.; Voigt-Martin, I.; Leibler, L. *Macromolecules* **1995**, *28*, 3080.
- Zheng, W.; Wang, Z.-G. *Macromolecules* **1995**, *28*, 7215.
- Dormidontova, E. E.; Khokhlov, A. R. *Macromolecules* **1997**, *30*, 1980.
- Mao, G.; Ober, C. K. *Acta Polym.* **1997**, *48*, 405.
- Fischer, H.; Poser, S. *Acta Polym.* **1996**, *47*, 413.
- Chen, J. T.; Thomas, E. L.; Ober, C. K.; Mao, G.-p. *Science* **1996**, *273*, 343.
- Chen, J. T.; Thomas, E. L.; Ober, C. K.; Hwang, S. S. *Macromolecules* **1995**, *28*, 1688.
- Stupp, S. I.; LeBonheur, V.; Walker, K.; Li, L. S.; Huggins, K. E.; Keser, M.; Amstutz, A. *Science* **1997**, *276*, 384.
- Adams, J.; Gronski, W. *Macromol. Chem., Rapid Commun.* **1989**, *10*, 553.
- Fischer, H.; Poser, S.; Arnold, M. *Liq. Cryst.* **1995**, *18*, 503.
- Yamada, M.; Iguchi, T.; Hirao, A.; Nakahama, S.; Watanabe, J. *Macromolecules* **1995**, *28*, 50.
- Bohnert, R.; Finkelmann, H. *Macromol. Chem. Phys.* **1994**, *195*, 689.
- Fischer, H.; Poser, S.; Arnold, M.; Frank, W. *Macromolecules* **1994**, *27*, 7133.
- Zaschke, B.; Frank, W.; Fischer, H.; Schmutzler, K.; Arnold, M. *Polym. Bull. (Berlin)* **1991**, *27*, 1.
- Angeloni, A. S.; Bignozzi, M. C.; Laus, M.; Chiellini, E.; Galli, G. *Polym. Bull. (Berlin)* **1993**, *31*, 387.
- Brehmer, M.; Mao, G.; Ober, C. K.; Zentel, R. *Makromol. Chem., Macromol. Symp.* **1997**, *117*, 175.
- Mao, G.; Wang, J.; Clingman, S. R.; Ober, C. K.; Chen, J. T.; Thomas, E. L. *Macromolecules* **1997**, *30*, 2556.
- Thomas, E. L.; Chen, J. T.; O'Rourke, M. J. E.; Ober, C. K.; Mao, G. *Macromol. Symp.* **1997**, *117*, 241.
- Bazuin, C. G.; Tork, A. *Macromolecules* **1995**, *28*, 8877.
- Navarro-Rodriguez, D.; Guillon, D.; Skoulios, A.; Frere, Y.; Gramain, P. *Macromol. Chem.* **1992**, *193*, 3117.
- Stewart, D.; Imrie, C. T. *Macromolecules* **1997**, *30*, 877.
- Kato, T.; Fréchet, J. M. J. *Macromolecules* **1989**, *22*, 3818.
- Kato, T.; Nakano, M.; Moteki, T.; Uryu, T.; Ujiie, S. *Macromolecules* **1995**, *28*, 8875.
- Ruokolainen, J.; Tanner, J.; ten Brinke, G.; Ikkala, O.; Torkkeli, M.; Serimaa, R. *Macromolecules* **1995**, *28*, 7779.
- Antonietti, M.; Conrad, J.; Thünemann, A. *Macromolecules* **1994**, *27*, 6007.
- Ikkala, O.; Ruokolainen, J.; ten Brinke, G.; Torkkeli, M.; Serimaa, R. *Macromolecules* **1995**, *28*, 7088.
- Antonietti, M.; Wenzel, A.; Thünemann, A. *Langmuir* **1996**, *12*, 2111.
- Antonietti, M.; Burger, C.; Thünemann, A. *Trends Polym. Sci.* **1997**, *5*, 262.
- Ober, C. K.; Wegner, G. *Adv. Mater.* **1997**, *9*, 17.
- Ruokolainen, J.; Torkkeli, M.; Serimaa, R.; Komanschek, E.; Ikkala, O.; ten Brinke, G. *Phys. Rev. E* **1996**, *54*, 6646.
- Ruokolainen, J.; Tanner, J.; Ikkala, O.; ten Brinke, G.; Thomas, E. L. *Macromolecules* **1998**, *31*, 3532.
- Ruokolainen, J.; Torkkeli, M.; Serimaa, R.; Komanschek, B. E.; ten Brinke, G.; Ikkala, O. *Macromolecules* **1997**, *30*, 2002.
- Ikkala, O.; Ruokolainen, J.; Torkkeli, M.; Tanner, J.; Serimaa, R.; ten Brinke, G. *Colloids Surf., A*, in press, 1998.
- Tal'roze, R. V.; Platé, N. A. *Polym. Sci.* **1994**, *36*, 1479.
- Tal'roze, R. V.; Kuptsov, S. A.; Sycheva, T. I.; Bezborodov, V. S.; Platé, N. A. *Macromolecules* **1995**, *28*, 8689.
- ten Brinke, G.; Ruokolainen, J.; Ikkala, O. *Europhys. Lett.* **1996**, *35*, 91.
- Luyten, M. C.; Alberda van Ekenstein, G. O. R.; ten Brinke, G.; Ruokolainen, J.; Ikkala, O.; Torkkeli, M.; Serimaa, R. *Macromolecules*, submitted for publication, 1998.

- (49) Huh, J.; Ikkala, O.; ten Brinke, G. *Macromolecules* **1997**, *30*, 1828.
- (50) Luyten, M. C.; Alberda van Ekenstein, G. O. R.; Wildeman, J.; ten Brinke, G.; Ruokolainen, J.; Ikkala, O.; Torkkeli, M.; Serimaa, R. *Macromolecules*, **1998**, *31*, 9160.
- (51) Fredrickson, G. H.; Leibler, L. *Macromolecules* **1989**, *22*, 1238.
- (52) Olvera de la Cruz, M. *J. Chem. Phys.* **1989**, *90*, 1995.
- (53) Whitmore, M. D.; Noolandi, J. *J. Chem. Phys.* **1990**, *93*, 2946.
- (54) Lodge, T. P.; Pan, C.; Jin, X.; Liu, Z.; Zhao, J.; Maurer, W. W.; Bates, F. S. *J. Polym. Sci., Part B: Polym. Phys.* **1995**, *33*, 2289.
- (55) Lodge, T. P.; Hamersky, M. W.; Hanley, K. J.; Huang, C.-I. *Macromolecules* **1997**, *30*, 6139.
- (56) Clarke, C. J.; Eisenberg, A.; La Scala, J.; Rafailovich, M. H.; Sokolov, J.; Li, Z.; Qu, S.; Nguyen, D.; Schwarz, S. A.; Strzhemechny, Y.; Sauer, B. B. *Macromolecules* **1997**, *30*, 4184.
- (57) Nyrkova, I. A.; Khokhlov, A. R.; Doi, M. *Macromolecules* **1993**, *26*, 3601.
- (58) Semenov, A. N. Unpublished results.
- (59) Sadron, C.; Gallot, B. *Makromol. Chem.* **1973**, *164*, 301.
- (60) Winey, K. I.; Thomas, E. L.; Fetters, L. J. *Macromolecules* **1992**, *25*, 2645.
- (61) Bates, F. S.; Schulz, M. F.; Khandpur, A. K.; Förster, S.; Rosedale, J. H.; Almdal, K.; Mortensen, K. *Faraday Discuss. Chem. Soc.* **1994**, *98*, 7.
- (62) Burger, C.; Micha, M. A.; Oestreich, S.; Förster, S.; Antonietti, M. *Europhys. Lett.* **1998**, *42*, 425.
- (63) Ruokolainen, J.; Ikkala, O.; ten Brinke, G. *Adv. Mater.*, submitted for publication, 1998.
- (64) Mäkinen, R.; Ruokolainen, J.; Ikkala, O.; de Moel, K.; ten Brinke, G.; De Odorico, W.; Stamm, M., to be published.

MA980189N